Inorganic Chemistry
Article

Inorg. Chem. **2009**, *48*, 11799–11808 **11799**
DOI: 10.1021/ic9018508

Coordination of N-Donor Ligands to a Uranyl(V) β-Diketiminate Complex

Michael F. Schettini, Guang Wu, and Trevor W. Hayton*

Department of Chemistry and Biochemistry, University of California Santa Barbara, Santa Barbara California, 93106

Received September 18, 2009

Addition of 2 equiv of AgOTf to $[UO_2(Ar_2nacnac)Cl]_2$ ($Ar_2nacnac=\{(2,6\text{-}Pr^i_2C_6H_3)NC(Me)\}_2CH$) in the presence of excess pyridine, followed by addition of Cp_2Co, generates the uranyl(V) complex $UO_2(Ar_2nacnac)(py)_2$ (**2**), in moderate yield. Complex **2** has proven to be an excellent precursor for the synthesis of other U(V) complexes. Thus, addition of 2,2′-bipyridine (bipy), 1,10-phenanthroline (phen), TMEDA, or 1-methylimidazole (MeIm) to **2** provides $UO_2(Ar_2nacnac)(bipy)$ (**3**), $UO_2(Ar_2nacnac)(phen)$ (**4**), $UO_2(Ar_2nacnac)(TMEDA)$ (**5**), and $UO_2(Ar_2nacnac)(MeIm)_2$ (**6**), respectively. Complexes **2**−**6** have been fully characterized and their structures confirmed by X-ray crystallography. Attempts to form the analogous hexavalent uranyl complexes of bipy, phen, and TMEDA have not been successful. However, reaction of $[UO_2(Ar_2nacnac)Cl]_2$ with AgOTf and 2 equiv of MeIm leads to the isolation of $[UO_2(Ar_2nacnac)(MeIm)_2][OTf]$ (**7**), which has been fully characterized. Attempts to ligate sulfur donor ligands to either the $UO_2(Ar_2nacnac)$ or the $[UO_2(Ar_2nacnac)]^+$ fragments were unsuccessful.

Introduction

The proposed scale-up of our nuclear energy capacity requires the development of highly efficient separations of the actinide ions from spent nuclear fuel (SNF), both to minimize waste and to facilitate actinide recycling back into the fuel cycle.[1,2] In addition, removal of long-lived transuranics, such as neptunium, from spent fuel has been suggested as a means of decreasing the thermal loading of the SNF repository, thereby increasing its capacity.[3] Efficient extraction of neptunium is also important because it exhibits appreciable mobility in groundwater, which provides it with a means of escaping long-term geological storage.[4−8] The well established PUREX process, which is based on the extractability of U(VI) and Pu(IV) with tributyl phosphate (TBP), permits the straightforward separation of uranium and plutonium.[1] In contrast, neptunium, which exists predominately as NpO_2^+ in aqueous aerobic conditions, is not efficiently complexed by TBP, and becomes fractioned between the product and the waste streams during the PUREX process.[2,9−11] It would be advantageous if Np(V) could be made readily extractable under conditions that are relevant to PUREX-type extractions. Unfortunately, the coordination chemistry of NpO_2^+ is not well understood,[1] making the design of ligands capable of complexing this ion a challenge.

Given the high radioactivity of Np^{237} ($t_{1/2} = 2.1 \times 10^6$ y), the use of a less hazardous analogue to model the reactivity of NpO_2^+ is an attractive opportunity. The isostructural pentavalent uranyl ion, namely, UO_2^+, is one potential analogue. However, its ability to model the chemistry of NpO_2^+ has not been verified, in part because UO_2^+ has proven troublesome to isolate.[12] In recent years however, several efficient synthetic routes to the UO_2^+ ion have been developed.[12,13] For example, UO_2^+ can be generated by oxidation of $UI_3(THF)_4$ with pyridine-*N*-oxide,[14−17] or through the reduction of UO_2^{2+}

*To whom correspondence should be addressed. E-mail: hayton@chem.ucsb.edu.

(1) *The Chemistry of the Actinide and Transactinide Elements*; Morss, L. R., Edelstein, N. M., Fuger, J., Katz, J. J., Eds.; Springer: New York, 2006.
(2) Madic, C.; Lecomte, M.; Baron, P.; Boullis, B. *C. R. Phys.* **2002**, *3*, 797–811.
(3) Todd, T. A.; Wigeland, R. A. *Advanced separation technologies for processing spent nuclear fuel and the potential benefits to a geologic repository*; Lumetta, G. J., Nash, K. L., Clark, S. B., Friese, J. I., Eds.; ACS Symposium Series 933; American Chemical Society: Washington, DC, 2006; pp 41−55.
(4) Gorden, A. E. V.; Xu, J.; Raymond, K. N.; Durbin, P. *Chem. Rev.* **2003**, *103*, 4207–4282.
(5) Kaszuba, J. P.; Runde, W. H. *Environ. Sci. Technol.* **1999**, *33*, 4427–4433.
(6) Ansoborlo, É.; Amekraz, B.; Moulin, C.; Moulin, V.; Taran, F.; Bailly, T.; Burgada, R.; Hengé-Napoli, M.-H.; Jeanson, A.; Den Auwer, C.; Bonin, L.; Moisy, P. *C. R. Chim.* **2007**, *10*, 1010–1019.
(7) Durbin, P. W.; Kullgren, B.; Xu, J.; Raymond, K. N.; Allen, P. G.; Bucher, J. J.; Edelstein, N. M.; Shuh, D. K. *Health Phys.* **1998**, *75*, 34–50.
(8) Taylor, D. M. *Sci. Total Environ.* **1989**, *83*, 217–225.
(9) Tian, G.; Xu, J.; Rao, L. *Angew. Chem., Int. Ed.* **2005**, *44*, 6200–6203.
(10) Tian, G.; Zhang, P.; Wang, J.; Rao, L. *Solv. Extr. Ion. Exch.* **2005**, *23*, 631–643.
(11) Taylor, R. J.; Denniss, I. S.; Wallwork, A. L. *Nuclear Energy* **1997**, *36*, 39–46.
(12) Arnold, P. L.; Love, J. B.; Patel, D. *Coord. Chem. Rev.* **2009**, *253*, 1973–1978.
(13) Graves, C. R.; Kiplinger, J. L. *Chem. Commun.* **2009**, 3831–3853.
(14) Burdet, F.; Pecaut, J.; Mazzanti, M. *J. Am. Chem. Soc.* **2006**, *128*, 16512–16513.
(15) Natrajan, L.; Burdet, F.; Pecaut, J.; Mazzanti, M. *J. Am. Chem. Soc.* **2006**, *128*, 7152–7153.
(16) Horeglad, P.; Nocton, G.; Filinchuk, Y.; Pecaut, J.; Mazzanti, M. *Chem. Commun.* **2009**, 1843–1845.

Published on Web 11/30/2009

Scheme 1

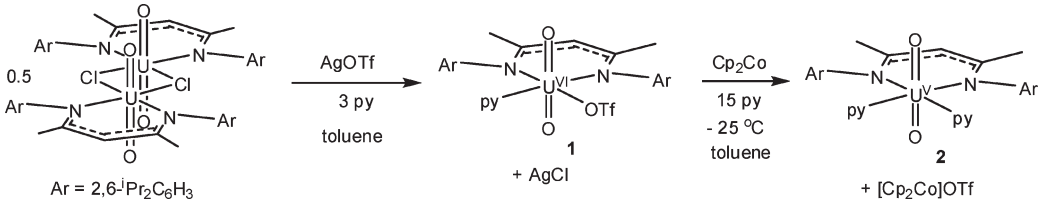

with KC_5R_5 (R = H, Me).[18,19] In addition, our laboratory has isolated several UO_2^+ complexes by reduction of uranyl(VI) β-diketiminates with $(C_5R_5)_2Co$ (R = H, Me).[20,21] The bulky aryl substituents of the β-diketiminate ligand offer steric protection to the uranyl(V) moiety, which kinetically stabilizes the 5+ state.

In this contribution we describe the synthesis and characterization of a new pentavalent uranyl β-diketiminate complex, $UO_2(Ar_2nacnac)(py)_2$ ($Ar_2nacnac$ = {(2,6-$Pr^i_2C_6H_3$)N-C(Me)}$_2$CH). This complex undergoes facile ligand exchange, allowing access to several new pentavalent uranyl derivatives. We also report the results of a competitive binding study with a series of nitrogen donor ligands, in an attempt to make predictions about the N-donor preference for Np(V).

Results

Synthesis of N-Donor Complexes. Reaction of $[UO_2(Ar_2nacnac)Cl]_2$ with 2 equiv of AgOTf in toluene results in the formation of a dull red solution. ^{1}H and ^{19}F NMR spectra of these solutions are consistent with the presence of $UO_2(Ar_2nacnac)(OTf)$, but attempts to isolate this material lead to the precipitation of an intractable red-brown powder, which is insoluble in toluene or CH_2Cl_2. Nonetheless, addition of excess pyridine to these solutions results in the formation of $UO_2(Ar_2nacnac)(py)(OTf)$ (**1**), which can be isolated as a polycrystalline solid in 57% yield (Scheme 1). Interestingly, even when a large excess of pyridine is added to the reaction mixture, the formation of a U(VI) bis(pyridine) complex is not observed.

Reduction of **1** with Cp_2Co at −25 °C, in the presence of 15 equiv of pyridine, generates $UO_2(Ar_2nacnac)(py)_2$ (**2**) and [Cp_2Co][OTf] (Scheme 1). The former can be isolated from toluene/hexane as purple prisms in 50% yield. The synthesis of **2** has proven to be quite sensitive to both temperature and stoichiometry. If fewer that 15 equiv of pyridine are used, or if the addition of Cp_2Co is not performed cold, the yields are substantially reduced. For example, if only 2 equiv of pyridine are used, then the reaction produces a significant amount of insoluble black solid, along with unreacted starting material. This black material may be UO_2,[22] formed by the over-reduction of **1**. It is worth noting that addition of Cp_2Co to a purified sample of **2** does not result in any reaction, as determined by ^{1}H NMR spectroscopy, which suggests that the black solid results from reduction of a coordinatively unsaturated species, such as "$UO_2(Ar_2nacnac)(py)$", generated along the reaction pathway to **2**. Complex **2** can also be synthesized in one pot, directly from $[UO_2(Ar_2nacnac)Cl]_2$, providing an overall yield of 69%.

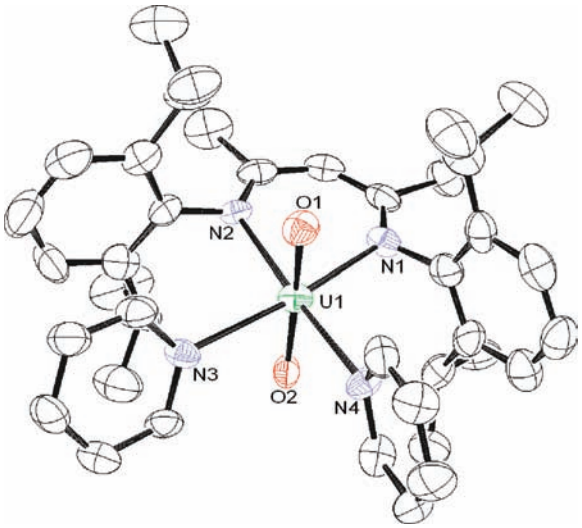

Figure 1. Solid state molecular structure of $UO_2(Ar_2nacnac)(py)_2 \cdot C_7H_8$ (**2**·C_7H_8) with thermal ellipsoids at the 50% probability level. Hydrogen atoms have been removed for clarity.

Table 1. Selected Bond Lengths (Å) and Angles (deg) for Complexes **2**−**6** and **7**

complex	**2**·C_7H_8	**3**·1/2C_7H_8	**4**	**5**	**6**·C_7H_8	**7**·CH_2Cl_2
U1−O1	1.792(6)	1.833(5)	1.819(5)	1.834(9)	1.76(1)	1.769(3)
U1−O2	1.797(6)	1.821(5)	1.834(5)	1.811(9)	1.762(9)	1.774(3)
U1−N1	2.484(7)	2.490(6)	2.493(6)	2.52(1)	2.55(1)	2.427(4)
U1−N2	2.515(7)	2.510(6)	2.506(6)	2.537(9)	2.51(1)	2.412(4)
U1−N3	2.627(8)	2.643(6)	2.643(6)	2.76(1)	2.61(1)	2.488(4)
U1−N4	2.609(8)	2.636(6)	2.639(7)	2.704(9)	2.58(2)	2.484(4)
O1−U1−O2	171.8(3)	175.9(2)	174.9(2)	172.0(4)	175.0(4)	175.4(2)
N1−U1−N4	108.9(3)	121.6(2)	121.8(2)	109.4(3)	99.1(4)	103.5(1)
N2−U1−N3	101.4(3)	105.1(2)	105.0(2)	109.9(3)	105.9(4)	106.9(1)

Complex **2** is highly soluble in toluene and benzene; however, it rapidly decomposes in CH_2Cl_2. Its ^{1}H NMR spectrum in C_6D_6 is consistent with the presence of the paramagnetic U^{5+} ion. For example, the two resonances assignable to the diastereotopic methyl protons of the isopropyl substituents are found at 17.14 ppm and −0.29 ppm, while the methine protons of the isopropyl substituents are observed at 14.75 ppm. X-ray quality crystals of **2** can be grown from a toluene/hexane solution. Complex **2** crystallizes in the monoclinic space group $P2_1/c$ as the toluene solvate **2**·C_7H_8, and its solid-state molecular structure is shown in Figure 1. Selected bond lengths and angles are found in Table 1. The uranium

(17) Nocton, G.; Horeglad, P.; Pecaut, J.; Mazzanti, M. *J. Am. Chem. Soc.* **2008**, *130*, 16633–16645.
(18) Berthet, J.-C.; Siffredi, G.; Thuery, P.; Ephritikhine, M. *Chem. Commun.* **2006**, 3184–3186.
(19) Berthet, J. C.; Siffredi, G.; Thuery, P.; Ephritikhine, M. *Dalton Trans.* **2009**, 3478–3494.
(20) Hayton, T. W.; Wu, G. *Inorg. Chem.* **2008**, *47*, 7415–7423.
(21) Hayton, T. W.; Wu, G. *J. Am. Chem. Soc.* **2008**, *130*, 2005–2014.
(22) McCleskey, T. M.; Foreman, T. M.; Hallman, E. E.; Burns, C. J.; Sauer, N. N. *Environ. Sci. Technol.* **2001**, *35*, 547–551.

center in **2** exhibits the expected octahedral geometry. The U−O(oxo) bond lengths in **2** (U−O = 1.792(6) Å and 1.797(6) Å) are typical of those observed for other pentavalent uranyl complexes;[12,14,15,18,20,21,23,24] however, the O−U−O angle (171.8(3)°) deviates significantly from the expected 180°. This may be due to an unfavorable steric interaction between the oxo ligands and the isopropyl substituents of the Ar_2nacnac ligand. Perturbations of the O−U−O angle in uranyl are usually small,[25] and are often the result of steric pressure, such as in $[Cp^*UO_2(CN)_3]^{2-}$ (168.40(9)°) and $UO_2(OAr)_2(thf)_2$ (Ar = 2,6-^{t}Bu$_2$C$_6$H$_3$) (167.8(4)°).[26,27] The U−N(nacnac) bond lengths are 2.484(7) Å and 2.515(7) Å, and fall within the range previously reported for uranyl(V)-Ar_2nacnac species.[20,21] The U−N(py) bond lengths are 2.627(8) Å and 2.609(8) Å, and are comparable to the U−N(py) bond lengths reported for $[UO_2(py)_5]^+$ (2.590(3) Å−2.612(3) Å).[15,18] Interestingly, one of the pyridine ligands (N4) is displaced out of the equatorial plane by 0.33(1) Å. Displacement of donor atoms out of the equatorial plane is uncommon for uranyl and usually require bulky, chelating ligands to be observed.[28−30] However, the out-of-plane deviation observed in complex **2** is not likely due to sterics, as the binding pocket of the $UO_2(Ar_2$nacnac) fragment appears to easily accommodate the two pyridine ligands.

Complex **2** is highly reactive, and even when stored as a solid at −25 °C it decomposes completely over the course of 2 weeks to a mixture containing H(Ar_2nacnac) and an insoluble brown precipitate. Nonetheless, **2** has proven to be a good starting material for the synthesis of other uranyl(V) complexes. For example, the addition of 1 equiv of 2,2′-bipyridine (bipy) to a toluene solution of **2** results in an immediate color change from purple to blue. From these solutions, $UO_2(Ar_2$nacnac)(bipy) (**3**) can be isolated in 80% yield (Scheme 2). Likewise, addition of 1 equiv of either 1,10-phenanthroline (phen) or TMEDA, or 2 equiv of 1-methylimidazole (MeIm), to solutions of **2** in toluene result in the formation of $UO_2(Ar_2$nacnac)(phen) (**4**), $UO_2(Ar_2$nacnac)(TMEDA) (**5**), or $UO_2(Ar_2$nacnac)(MeIm)$_2$ (**6**), respectively, in moderate to excellent yields (Scheme 2).

Like **2**, complexes **3**−**6** are soluble in toluene and benzene, while **5** is also soluble in hexanes. These materials are highly sensitive to air and moisture and they quickly decompose in the presence of dichloromethane. In addition, complexes **3**,**4** and **6** are also temperature sensitive. Solutions of these compounds in C_6D_6 decompose completely over the course of 24 h. In contrast, complex **5** has proven to be reasonably thermally stable,

Scheme 2

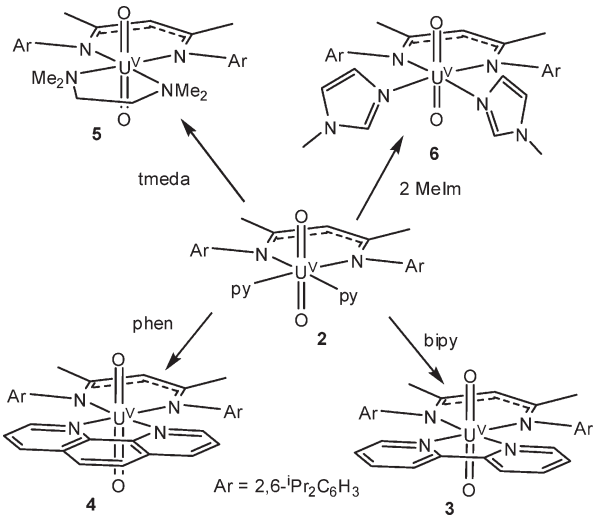

showing no sign of decomposition after 3 days in C_6D_6 at room temperature.

The ^{1}H NMR spectra of **3**−**6** in C_6D_6 are consistent with the presence of the paramagnetic uranyl(V) ion. For example, in complex **3** the diastereotopic methyl groups of the isopropyl substituents are observed at 17.39 ppm and 0.25 ppm as broad singlets, while the methyl groups attached to the β-carbons of the Ar_2nacnac backbone are observed at −8.94 ppm. The presence of bipy is confirmed by a singlet at −44.59 ppm, assignable to the protons at the 6-position of the bipy fragment.

The UV/vis spectra of complexes **2**−**6** are also consistent with the presence of the $5f^1$ ion and exhibit weak absorptions assignable to f→f transitions (Figure 2). For example, complex **2** exhibits an absorption at 781 nm (ε = 290 L·mol^{-1}·cm^{-1}), while **6** exhibits an absorption at 758 nm (ε = 150 L·mol^{-1}·cm^{-1}). Interestingly, the UV/vis spectra for complexes **3**−**5** are reasonably comparable (Figure 2), probably because of their structural similarity. All spectra are qualitatively similar to those previously reported for uranyl(V) Ar_2nacnac complexes.[20,21]

The IR spectra of complexes **2**−**6** were also obtained. Complex **2** exhibits a vibration at 811 cm^{-1}, which we have assigned to ν_{asym}(U=O). Similarly, the IR spectra of complexes **3**−**6** exhibit vibrations at 819 cm^{-1}, 816 cm^{-1}, 820 cm^{-1}, and 810 cm^{-1}, respectively, which were also assigned to ν_{asym}(U=O). These values are consistent with those reported for other uranyl(V) complexes.[14−17,21,31]

We have also attempted to ligate several sulfur donors to the $UO_2(Ar_2$nacnac) fragment. Addition of excess Ph_2MePS to a solution of **2** in C_6D_6 results in no change to its ^{1}H NMR spectrum. Likewise, addition of Ph_2MePS to a solution of $UO_2(Ar_2$nacnac)$(Ph_2MePO)_2$[21] in C_6D_6 results in no observable change. Similar results are found with Ph_3PS, $\{Ph_2PS\}_2CH_2$, thiophene, and tetrahydrothiophene.

Solid-State Molecular Structures. Given the rarity of isolable pentavalent uranyl complexes, we have undertaken a structural study of complexes **3**−**6**, in an attempt to further understand the structure of this class of molecules. Crystals of **3**, **4**, and **6**, suitable for X-ray diffraction

(23) Berthet, J.-C.; Nierlich, M.; Ephritikhine, M. *Angew. Chem., Int. Ed.* **2003**, *42*, 1952–1954.
(24) Hayton, T. W.; Wu, G. *Inorg. Chem.* **2009**, *48*, 3065–3072.
(25) Alcock, N. W.; Flanders, D. J.; Brown, D. *Dalton Trans.* **1984**, 679–681.
(26) Maynadie, J.; Berthet, J.-C.; Thuery, P.; Ephritikhine, M. *Chem. Commun.* **2007**, 486–488.
(27) Wilkerson, M. P.; Burns, C. J.; Morris, D. E.; Paine, R. T.; Scott, B. L. *Inorg. Chem.* **2002**, *41*, 3110–3120.
(28) Berthet, J.-C.; Nierlich, M.; Ephritikhine, M. *Dalton Trans.* **2004**, 2814–2821.
(29) Berthet, J.-C.; Nierlich, M.; Ephritikhine, M. *Chem. Commun.* **2003**, 1660–1661.
(30) Sarsfield, M. J.; Helliwell, M.; Raftery, J. *Inorg. Chem.* **2004**, *43*, 3170–3179.
(31) Mizuoka, K.; Ikeda, A. *Inorg, Chem.* **2003**, *42*, 3396–3398.

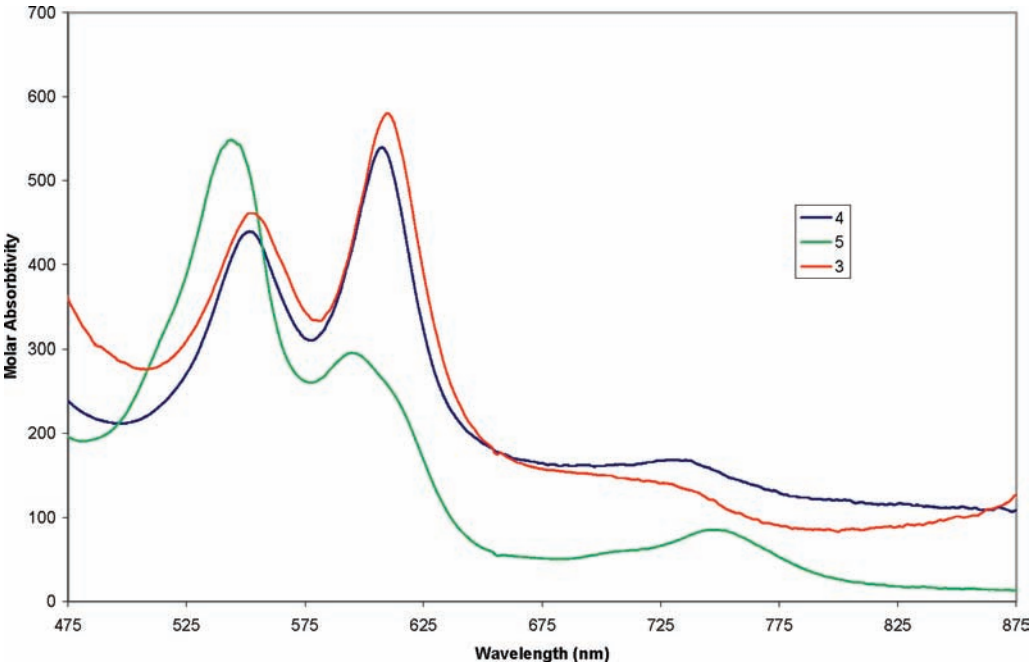

Figure 2. Room temperature UV−vis spectra of **3** (1.4 mM, toluene), **4** (1.1 mM, toluene), and **5** (3.8 mM, toluene).

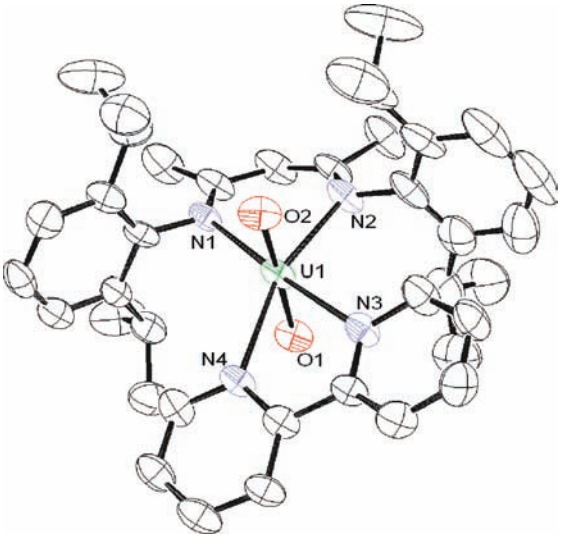

Figure 3. Solid state molecular structure of $UO_2(Ar_2nacnac)(bipy)\cdot 1/2C_7H_8$ (**3**·$1/2C_7H_8$) with thermal ellipsoids at the 50% probability level. Hydrogen atoms have been removed for clarity.

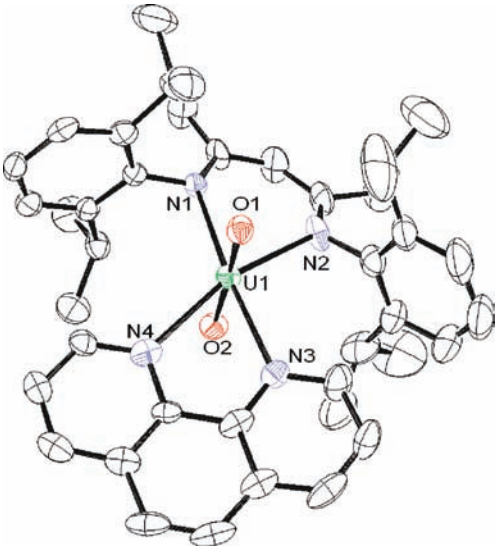

Figure 4. Solid state molecular structure of $UO_2(Ar_2nacnac)(phen)$ (**4**) with thermal ellipsoids at the 50% probability level. Hydrogen atoms have been removed for clarity.

were grown from toluene/hexane solutions at −25 °C, while crystals of **5** were grown from a concentrated hexane solution at −25 °C. Under these conditions complexes **3** and **6** crystallize as the toluene solvates, **3**·$1/2C_7H_8$ and **6**·C_7H_8, respectively. The solid-state molecular structures of complexes **3**−**6** are shown in Figures 3−6, respectively. Selected bond length and angles for **3**·$1/2C_7H_8$, **4**, **5**, and **6**·C_7H_8 can be found in Table 1. For each complex, the uranium center exhibits a distorted octahedral geometry, and in complexes **3**·$1/2C_7H_8$ and **4**, one of the N atoms of polypyridyl ligand is notably displaced out of the equatorial plane. In complex **3**, N4 is displaced by 0.54(1) Å out of the equatorial plane, while for **4**, N4 is displaced by 0.42(1) Å out of the equatorial plane. The asymmetry of bipy and phen binding is further revealed by comparing the N2−U1−N3 (**3**: 105.1(2)°; **4**: 105.0(2)°) and N1−U1−N4 (**3**: 121.6(2)°; **4**: 121.8(2)°) angles, which differ by 16°. This deviation from octahedral geometry is likely due to crystal packing, as both complexes exhibit intermolecular π-stacking between the polypyridyl rings in their solid-state molecular structures. Nonetheless, the observation of out-of-plane interactions in three of the five U(V) complexes characterized in this study (i.e., complexes **2**, **3**, and **4**) suggests that such deviations may be less energetically costly in pentavalent uranyl than they are in hexavalent uranyl.

In complexes **3** and **4**, the metrical parameters for the UO_2^+ fragment closely resemble those of previously reported uranyl(V) complexes.[14,15,18,20,21,23] For

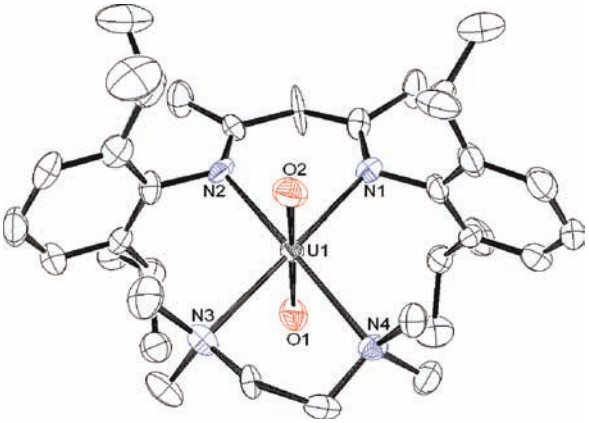

Figure 5. Solid state molecular structure of $UO_2(Ar_2nacnac)(TMEDA)$ (**5**) with thermal ellipsoids at the 50% probability level. Hydrogen atoms have been removed for clarity.

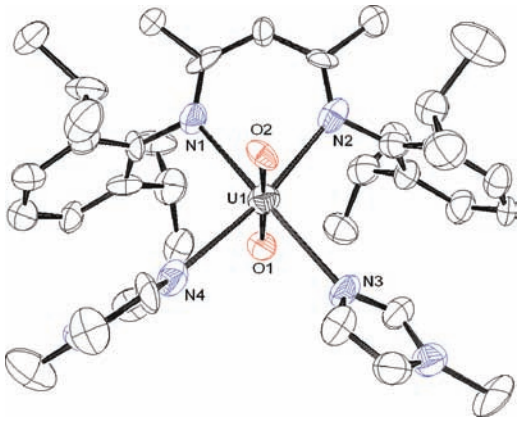

Figure 6. Solid state molecular structure of $UO_2(Ar_2nacnac)(MeIm)_2 \cdot C_7H_8$ (**6**$\cdot C_7H_8$) with thermal ellipsoids at the 50% probability level. Hydrogen atoms have been removed for clarity.

example, the U−O(oxo) bonds (**3**: U−O = 1.821(5) Å and 1.833(5) Å; **4**: U−O = 1.819(5) Å and 1.834(5) Å) are slightly longer than those normally observed for hexavalent uranyl (ca. 1.76 Å),[32,33] while the O−U−O angles are approximately linear (**3**: 175.9(2)°; **4**: 174.9(2)). In complex **5**, the O−U−O angle (O1−U1−O2 = 172.0(4)°) is similar to that observed for **2**, while in complex **6**, the uranyl moiety exhibits U−O bond lengths (U1−O2 = 1.762(9) Å and U1−O1 = 1.76(1) Å) closer to those expected for uranyl(VI). The longer U−O bonds in **3**, **4**, and **5**, relative to U(VI), are in agreement with the low ν_{asym}(UO) values observed in their IR spectra (vide supra).

The U−N(bipy) bond lengths in **3** are 2.636(6) Å and 2.643(6) Å, while the U−N(phen) bond lengths in **4** are 2.643(6) Å and 2.639(7) Å. These values are comparable to the U−N(py) bond lengths exhibited by **2**, and are within the range previously reported for uranyl(VI) polypyridyl complexes (2.47(3) Å−2.688(4) Å).[34−40] The U−N(TMEDA) bond lengths in **5** are U1−N4 = 2.704(9) Å and U1−N3 = 2.76(1) Å, notably longer than the U−N bonds in the bipy and phen adducts. Finally, the U−N-(MeIm) bond lengths in **6** are 2.61(1) Å and 2.58(2) Å, and are comparable to the U−N(MeIm) bond lengths observed in $UO_2(Ac)_2(MeIm)_2$ (2.528(3) Å).[41]

Table 2. Relative Ratios of Product and Reactants Formed upon Addition of Neutral N-Donor Ligands to Complexes **2**−**6**[a]

complex	incoming ligand	product	reactant/product ratio
2	bipy	**3**	complete conversion
2	phen	**4**	complete conversion
2	TMEDA	**5**	complete conversion
2	MeIm	**6**	complete conversion
3	phen	**4**	complete conversion
3	TMEDA	**5**	1:2.5
3	MeIm	**6**	complete conversion
4	bipy	**3**	no conversion
4	TMEDA	**5**	16:1
4	MeIm	**6**	2.2:1
5	bipy	**3**	3:1
5	phen	**4**	1:13
5	MeIm	**6**	1:4.6
6	bipy	**3**	no conversion
6	phen	**4**	1:2.5
6	TMEDA	**5**	6.5:1

[a] All reactions were performed by addition of 1 equiv of incoming ligand (or 2 equiv if a monodentate ligand).

Competition Experiments. With our suite of nitrogen donor complexes in hand we have attempted to rank the binding ability of the five N-donor ligands via a series of competition experiments. These experiments were performed by addition of an equimolar amount of incoming ligand (or twice the equimolar amount for MeIm) to a approximately 0.02 M C_6D_6 solution of complexes **3**, **4**, **5**, and **6**. Ligand preference was determined by recording the ^{1}H NMR spectrum and calculating the product/reactant ratio. Every ligand/complex combination was monitored in this fashion. This qualitative approach was chosen because the slow decomposition of these temperature sensitive complexes made the calculation of a quantitative equilibrium constant challenging. Generally, over the course of the experiment, decomposition amounted to less than 5% of the sample. It should also be noted that ligand exchange occurred essentially instantaneously for all ligand/complex combinations.

The data for ligand preference are shown in Table 2. In several instances complete conversion was observed. For example, upon addition of an equimolar amount of phen to a solution of **3** in C_6D_6, complete conversion to complex **4** occurs, as determined by ^{1}H NMR spectroscopy. A similar result is observed upon addition of 2 equiv of MeIm to complex **3**. On the basis of the data presented in Table 2, we have ranked the ligand binding

(32) Denning, R. G. *J. Phys. Chem. A* **2007**, *111*, 4125–4143.
(33) Denning, R. G. *Struct. Bonding* (*Berlin*) **1992**, *79*, 215–276.
(34) Alcock, N. W.; Flanders, D. J.; Brown, D. *Inorg. Chim. Acta* **1984**, *94*, 279–282.
(35) Deacon, G. B.; Mackinnon, P. I.; Taylor, J. C. *Polyhedron* **1985**, *4*, 103–113.
(36) Panchanan, S.; Hamalainen, R.; Roy, P. S. *J. Chem. Soc., Dalton Trans.* **1994**, 2381–2390.
(37) Alcock, N. W.; Flanders, D. J.; Pennington, M.; Brown, D. *Acta Crystallogr.* **1988**, *C44*, 247–250.
(38) Berthet, J.-C.; Nierlich, M.; Ephritikhine, M. *Chem. Commun.* **2003**, 1660–1661.
(39) Das, S.; Madhavaiah, C.; Verma, S.; Bharadwaj, P. K. *Inorg. Chim. Acta* **2006**, *359*, 548–552.
(40) Jiang, Y.-S.; Yu, Z.-T.; Liao, Z.-L.; Li, G.-H.; Chen, J.-S. *Polyhedron* **2006**, *25*, 1359–1366.
(41) Gutowski, K. E.; Cocalia, V. A.; Griffin, S. T.; Bridges, N. J.; Dixon, D. A.; Rogers, R. D. *J. Am. Chem. Soc.* **2007**, *129*, 526–536.

Scheme 3

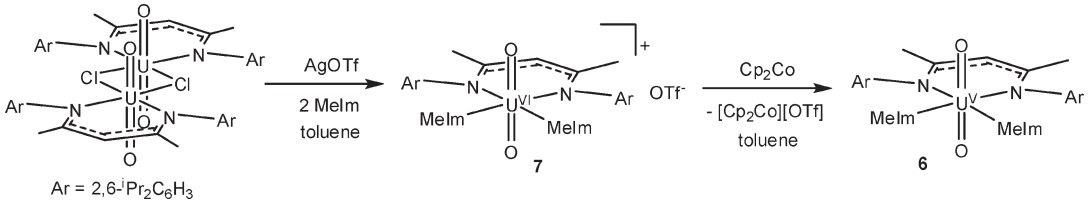

preference of the $UO_2(Ar_2nacnac)$ fragment in the following fashion: phen > MeIm > TMEDA > bipy > py.

Comparison with Hexavalent Uranyl. To compare the above results with U(VI), we have also explored the ability of the isostructural hexavalent uranyl fragment, $[UO_2(Ar_2nacnac)]^+$, to coordinate N-donor ligands. In situ generation of $UO_2(Ar_2nacnac)(OTf)$ in CD_2Cl_2 followed by addition of TMEDA results in no reaction, while addition of phen or bipy to $UO_2(Ar_2nacnac)(OTf)$ generates intractable mixtures. Analysis of these latter mixtures by ^1H NMR spectroscopy reveals that free ligand and unreacted $UO_2(Ar_2nacnac)(OTf)$ are the major products. Several minor unidentified products are also present. When bipy, phen or TMEDA is added to $[UO_2(Ar_2nacnac)(Ph_2MePO)_2][OTf]$,[21] no displacement of Ph_2MePO is observed. Coordination of pyridine to $[UO_2(Ar_2nacnac)(Ph_2MePO)_2][OTf]$ can be effected, but only upon addition of 20 equiv of pyridine. ^1H NMR spectra of these samples reveal the formation of a mixed ligand complex, namely, $[UO_2(Ar_2nacnac)(Ph_2MePO)(py)][OTf]$ (See Supporting Information). Attempts to coordinate Ph_2MePS to $[UO_2(Ar_2nacnac)]^+$ were also unsuccessful, regardless of the solvent employed or the counterion used (either OTf^- or BF_4^-).

In contrast to the above results, addition of 2 equiv of MeIm to $UO_2(Ar_2nacnac)(OTf)$ results in immediate formation of $[UO_2(Ar_2nacnac)(MeIm)_2][OTf]$ (**7**) (Scheme 3), which can be isolated in good yield as a maroon crystalline solid. Complex **7** is soluble in toluene and dichloromethane. Its ^1H NMR spectrum in CD_2Cl_2 contains a singlet at 3.65 ppm, assignable to the methyl group of the MeIm ligand. The diastereotopic methyl protons of its isopropyl substituents are observed as doublets at 0.82 ppm and 1.18 ppm. Complex **7** can also be reduced with Cp_2Co, forming **6** in moderate yield (Scheme 3).

X-ray quality crystals of **7** were grown from solutions of dichloromethane/hexane. Complex **7** crystallizes in the monoclinic space group $P2_1/n$, as a dichloromethane solvate, $\mathbf{7}\cdot CH_2Cl_2$, and its solid-state molecular structure is shown in Figure 7. The oxo ligands of **7** exhibit metrical parameters typical of the uranyl(VI) moiety (U−O = 1.769(3) Å and 1.774(3) Å, ∠O−U−O = 175.4(2)°). Its U−N(MeIm) bond lengths (2.488(4) Å and 2.484(4) Å) are slightly shorter than those of the other structurally characterized uranyl(VI)-imidazole complex (U−N(MeIm) = 2.528(3) Å).[41] By the 3σ criteria the U−O(oxo) bond lengths of **7** and **6** are identical (see Table 1). However, the U−N(nacnac) and U−N(MeIm) bond lengths of **7** are shorter than those of **6**, as expected for the smaller ionic radius of the U^{6+} ion. As with all the uranyl complexes reported in this study, the aryl substituents of the $Ar_2nacnac$ ligand in both **6** and **7** are tilted toward the uranyl ion. For example, the U−C(ipso) distances in **7** are

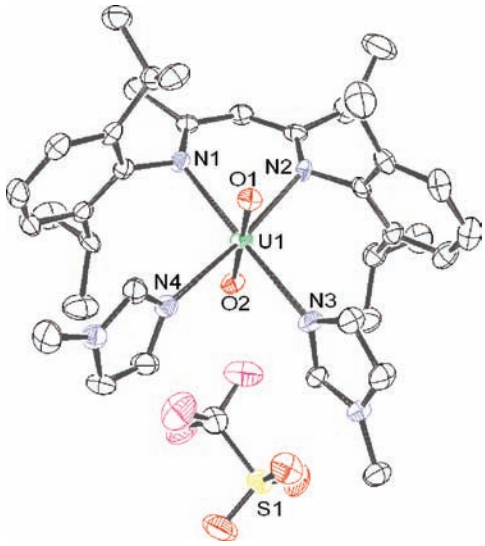

Figure 7. Solid state molecular structure of $[UO_2(Ar_2nacnac)(MeIm)_2][OTf]\cdot CH_2Cl_2$ ($\mathbf{7}\cdot CH_2Cl_2$) with thermal ellipsoids at the 50% probability level. Hydrogen atoms have been removed for clarity.

U1−C1 = 3.067(5) Å and U1−C18 = 2.998(5) Å, while the U−C(ipso) distances in **6** are 3.22(2) Å and 3.20(2) Å. This amounts to a difference of only 6%, suggesting that the steric profile of the $Ar_2nacnac$ ligand is not greatly affected by the uranium oxidation state.

Complex **7** can also be prepared by addition of excess MeIm to $[UO_2(Ar_2nacnac)(Ph_2MePO)_2][OTf]$; however a mixed ligand complex, namely $[UO_2(Ar_2nacnac)(Ph_2MePO)(MeIm)][OTf]$ (**8**), is the major product in the reaction mixture according to ^1H NMR spectroscopy. Complex **8** can also be prepared by addition of 2 equiv of Ph_2MePO and 2 equiv of MeIm to $UO_2(Ar_2nacnac)(OTf)$, where it can be isolated in moderate yield. Consistent with the proposed structure, its ^1H NMR spectrum exhibits a doublet at 1.85 ppm, assignable to the methyl group of the Ph_2MePO ligand. Also present is a singlet at 3.53 ppm, assignable to the methyl group of the MeIm ligand. The ^{31}P NMR spectrum of **7** exhibits a singlet at 51.68 ppm in C_6D_6. For comparison, the free ligand appears at −9.36 ppm in C_6D_6. Its solid state molecular structure has also been determined, and full details can be found in the Supporting Information.

Discussion

The ability of the $Ar_2nacnac$ ligand to stabilize the UO_2^+ fragment, while only occupying two equatorial ligand sites, provides us with an opportunity to explore the ligand exchange chemistry of this normally unstable moiety. We have found that the $UO_2(Ar_2nacnac)$ fragment will readily coordinate nitrogen-donor ligands, and we have structurally characterized a series of pentavalent uranyl complexes

containing common N-donor ligands. We have also determined the relative binding ability of these five ligands to $UO_2(Ar_2nacnac)$. Of the monodentate ligands tested, 1-methylimidazole was preferred over pyridine, consistent with the pK_b values of these two bases,[42] while S-donors (such as Ph_2MePS, thiophene, and tetrahydrothiophene) exhibited no propensity to coordinate UO_2^+. For the bidentate N-donors, phen was found to displace both TMEDA and bipy, while TMEDA could displace bipy. The binding preference of phen over bipy is consistent with previously observed selectivity for these two ligands, and relates to smaller reorganization energy required for phen to bind a metal ion.[43,44] The ability of TMEDA to outcompete bipy may be due to its higher Brønstead basicity,[42] a rationale that has been invoked previously.[45] However, the higher selectivity may also be due to the smaller steric profile of TMEDA versus bipy. On the basis of the solid state molecular structure of **3** there appears to be an unfavorable steric interaction between the aryl ring of the $Ar_2nacnac$ ligand and the proton at the 6-position of the bipy ring. As a result, TMEDA may exhibit a better fit within the relatively constricted binding pocket of $UO_2(Ar_2nacnac)$. A similar rationale could account for the observation that the monodentate MeIm ligand can outcompete both TMEDA and bipy. In this case, the MeIm ring binds parallel to the aryl substitutent of the $Ar_2nacnac$ ligand which may result in less steric repulsion, relative to TMEDA and bipy. The better steric match could be enough to counteract the unfavorable entropic effect commensurate upon displacement of a bidentate ligand.

To provide context for our U(V) results we have also explored the interaction of these N-donor ligands with the isostructural $[UO_2(Ar_2nacnac)]^+$ fragment. For U(VI), the monodentate ligands 1-methylimidazole and pyridine were the only N-donors capable of coordinating to the $[UO_2(Ar_2nacnac)]^+$ fragment. Surprisingly, none of the bidentate N-donors we examined would bind to $[UO_2(Ar_2nacnac)]^+$ under any conditions.

Overall, these results demonstrate that the pentavalent $UO_2(Ar_2nacnac)$ fragment has an increased ability to coordinate N-donors, relative to hexavalent $[UO_2(Ar_2nacnac)]^+$. Preliminary coordination and extraction studies with other AnO_2^+ ions are consistent with this finding. For example, the tetradentate N-donor 6,6′-bis(5,6-dialkyl-1,2,4-triazin-3-yl)bipyridine (BTBP) can extract NpO_2^+ from 1 M HNO_3, whereas it does not extract UO_2^{2+} under similar conditions.[46] Other N-donor ligands such as bipy,[47,48] phen,[49] imidazole,[50] and tptz (2,4,6-tri-(2-pyridin-2-yl)-1,3,5,-triazine)[51] are also able to coordinate aqueous pentavalent neptunyl. These results are consistent with the large body of literature concerning the use of nitrogen-based heterocycles to preferentially coordinating the softer An^{3+} ions over the hard Ln^{3+} ions.[52] The general bonding rationale supporting the use of these ligands is that the 5f and 6d orbitals are sufficiently spatially extended to participate in covalent interactions, which favor polarizable donor atoms, such as N and S.[53−57] A similar effect may be operative in UO_2^+, where the lower charge, relative to UO_2^{2+}, could result in an expansion of the orbitals involved in equatorial ligand bonding, rendering the coordination of softer nitrogen-based ligands more favorable.[9]

Summary

We have investigated the ability of UO_2^+ to coordinate a series of N-donor and S-donor ligands. We have found that the $UO_2(Ar_2nacnac)$ fragment binds a variety of N-donors, such as bipy, TMEDA, phen, and MeIm. In contrast, we have found that the isostructural U^{6+} fragment, $[UO_2(Ar_2nacnac)]^+$, does not readily coordinate these N-donor ligands (with the exception of MeIm). This difference may be due to higher polarizability of the U^{5+} ion, making the coordination of nitrogen donors more favorable, relative to the U^{6+} ion. The enhanced ability to coordinate nitrogen donors may also exist for the other actinyl(V) ions, such as NpO_2^+, and may explain why NpO_2^+ is not extracted out of the aqueous phase during the PUREX process (a system designed to extract the hard hexavalent AnO_2^{2+} ions and tetravalent An^{4+} ions).[11,58,59] Future studies will attempt to extend this work to pentavalent neptunyl with the eventual goal of determining the ligand preference for this moiety.

Experimental Section

General Procedures. All reactions and subsequent manipulations were performed under anaerobic and anhydrous conditions either under high vacuum or an atmosphere of nitrogen or argon. Hexanes, diethyl ether and toluene were dried by passage over activated molecular sieves using a Vacuum Atmospheres solvent purification system. Tetrahydrofuran (THF) was either distilled from Na/benzophenone before use or dried by passage over activated molecular sieves using a Vacuum Atmospheres solvent purification system. Pyridine was distilled from CaH_2 before use. C_6D_6 and MeIm were dried over activated 4 Å molecular sieves, while CH_2Cl_2 and CD_2Cl_2 were dried over activated 3 Å molecular sieves for 24 h. $UO_2Cl_2(THF)_3$,[60] $Li(Ar_2nacnac)$,[61] $[UO_2(Ar_2nacnac)Cl]_2$,[21] and $[UO_2(Ar_2nacnac)(Ph_2MePO)_2][OTf]$[21] were prepared by the published

(42) Perrin, D. D. *Stability Constants of Metal-Ion Complexes, Part B: Organic Ligands*; Permagon Press: New York, 1982.
(43) Tsierkezos, N. G.; Diefenbach, M.; Roithova, J.; Schroder, D.; Schwarz, H. *Inorg. Chem.* **2005**, *44*, 4969–4978.
(44) Davydova, E. I.; Sevastianova, T. N.; Timoshkin, A. Y.; Suvorov, A. V.; Frenking, G. *Int. J. Quantum Chem.* **2004**, *100*, 419–425.
(45) Condike, G. F.; Martell, A. E. *J. Inorg. Nucl. Chem.* **1969**, *31*, 2455–2466.
(46) Retegan, T.; Ekberg, C.; Dubois, I.; Fermvik, A.; Skarnemark, G.; Wass, T. J. *Solv. Extr. Ion Exch.* **2007**, *25*, 417–431.
(47) Andreev, G. B.; Fedosseev, A. M.; Budantseva, N. A.; Antipin, M. Y. *Mendeleev Commun.* **2001**, *11*, 58–59.
(48) Andreev, G. B.; Budantseva, N. A.; Tananaev, I. G.; Myasoedov, B. F. *Inorg. Chem. Commun.* **2009**, *12*, 109–111.
(49) Budantseva, N. A.; Andreev, G. B.; Fedoseev, A. M.; Antipin, M. Y. *Koord. Khim.* **2003**, *29*, 346–350.
(50) Andreev, G. B.; Budantseva, N. A.; Tananaev, I. G.; Myasoedov, B. F. *Inorg. Chem.* **2009**, *48*, 1232–1235.
(51) Budantseva, N. A.; Andreev, G. B.; Fedosseev, A. M.; Bessonov, A. A.; Antipin, M. Y.; Krupa, J.-C. *C. R. Chim.* **2005**, *8*, 91–95.
(52) Kolarik, Z. *Chem. Rev.* **2008**, *108*, 4208–4252.
(53) Gaunt, A. J.; Reilly, S. D.; Enriquez, A. E.; Scott, B. L.; Ibers, J. A.; Sekar, P.; Ingram, K. I. M.; Kaltsoyannis, N.; Neu, M. P. *Inorg. Chem.* **2008**, *47*, 29–41.
(54) Mazzanti, M.; Wietzke, R.; Pecaut, J.; Latour, J. M.; Maldivi, P.; Remy, M. *Inorg. Chem.* **2002**, *41*, 2389–2399.
(55) Jensen, M. P.; Bond, A. H. *J. Am. Chem. Soc.* **2002**, *124*, 9870–9877.
(56) Choppin, G. R. *J. Alloys Compd.* **2002**, *344*, 55–59.
(57) Petit, L.; Adamo, C.; Maldivi, P. *Inorg. Chem.* **2006**, *45*, 8517–8522.
(58) *Solvent Extraction Principles and Practice*. 2nd ed.; Rydberg, J., Cox, M., Musikas, C., Choppin, G. R., Eds.; Marcel Dekker, Inc.: New York, 2004.
(59) *Handbook of Solvent Extraction*; Lo, T. C., Baird, M. H. I., Hanson, C., Eds.; John Wiley & Sons: New York, 1983.
(60) Wilkerson, M. P.; Burns, C. J.; Paine, R. T.; Scott, B. L. *Inorg. Chem.* **1999**, *38*, 4156–4158.
(61) Stender, M.; Wright, R. J.; Eichler, B. E.; Prust, J.; Olmstead, M. M.; Roesky, H. W.; Power, P. P. *J. Chem. Soc., Dalton Trans.* **2001**, 3465–3469.

procedures. Ph_2MePS was prepared by reaction of Ph_2MeP with sulfur in THF at room temperature.[62] Cp_2Co was recrystallized from CH_2Cl_2/hexanes. All other reagents were purchased from commercial sources and used as received.

NMR spectra were recorded on a Varian INOVA 400 or a Varian UNITY INOVA 500 spectrometer. ^1H and $^{13}C\{^1H\}$ NMR spectra are referenced to external $SiMe_4$ using the residual protio solvent peaks as internal standards (^1H NMR experiments) or the characteristic resonances of the solvent nuclei (^{13}C NMR experiments). $^{31}P\{^1H\}$ NMR spectra were referenced to external 85% H_3PO_4, while $^{19}F\{^1H\}$ NMR spectra were referenced to external α,α,α-trifluorotoluene. Elemental analyses were performed by the Microanalytical Laboratory at UC Berkeley. UV/vis spectra were recorded on an Ocean Optics USB4000 UV/vis spectrometer equipped with a USB-DT light source. IR spectra were recorded on a Mattson Genesis FTIR spectrometer.

Synthesis of UO_2(Ar$_2$nacnac)(OTf)(py) (1). To a toluene solution (10 mL) of $[UO_2(Ar_2nacnac)Cl]_2$ (91 mg, 0.063 mmol) was added AgOTf (36 mg, 0.14 mmol). The color of the solution quickly changed from green-brown to dull-red concomitant with the deposition of a white powder. After 30 min of stirring, the solution was filtered through a Celite column (2 cm × 0.5 cm) supported on glass wool. Pyridine (30 μL, 0.38 mmol) was added to the filtrate, and the resulting orange-brown solution was filtered through a Celite column (2 cm × 0.5 cm) supported on glass wool. The volume of filtrate was reduced in vacuo (0.5 mL), and the solution was layered with hexanes (4 mL) and stored at −25 °C for 12 h. This resulted in the deposition of an orange-brown polycrystalline solid (66 mg). Yield: 57%. Anal. Calcd for $C_{35}H_{46}N_3SF_3O_5U$: C, 45.90; H, 5.06; N, 4.59. Found C, 45.76; H, 4.82; N, 4.39. ^1H NMR (400 MHz, 25 °C, C_6D_6): δ 0.69 (d, 6H, J_{HH} = 6.4 Hz, CH*Me*$_2$), 0.96 (d, 6H, J_{HH} = 7.6 Hz, CH*Me*$_2$), 1.14 (d, 6H, J_{HH} = 6.0 Hz, CH*Me*$_2$), 1.19 (d, 6H, J_{HH} = 6.8 Hz, CH*Me*$_2$), 1.92 (s, 6H, Me), 3.62 (m, 4H, C*H*Me$_2$), 4.72 (s, 1H, γ CH), 6.53 (t, 1H, J_{HH} = 7.2 Hz, *para* CH, py), 6.69 (t, 2H, J_{HH} = 5.6 Hz, *meta* CH), 6.78 (d, 2H, J_{HH} = 7.6 Hz, *meta* CH), 6.92 (t, 1H, J_{HH} = 5.6 Hz, *para* CH), 7.44 (d, 1H, J_{HH} = 3.6 Hz, *para* CH), 7.51 (d, 2H, J_{HH} = 3.4 Hz, *meta* CH, py), 8.42 (d, 2H, J_{HH} = 4.0 Hz, *ortho* CH, py). $^{19}F\{^1H\}$ NMR (376 MHz, 25 °C, C_6D_6): δ −14.33 (s, OTf). $^{13}C\{^1H\}$ NMR (125 MHz, 25 °C, C_6D_6): δ 23.51 (Me), 24.42 (Me), 26.68 (CH*Me*$_2$), 26.83 (CH*Me*$_2$), 27.81 (CH*Me*$_2$), 27.93 (CH*Me*$_2$), 28.34 (*C*HMe$_2$), 28.48 (*C*HMe$_2$), 98.76 (γ-C), 125.02, 125.06, 126.91, 130.56, 131.49, 132.35, 133.65, 139.47, 149.75 (2-py), 150.66 (C ipso), 151.40 (C ipso), 166.40 (β-C), 167.66 (β-C). A resonance for the CF_3 group was not observed. IR (KBr Pellet, cm^{-1}): 1338(m), 1318(s), 1279(s), 1239(s), 1200(s), 1178(s), 1104(w), 1031(m), 1015(m), 1012(sh), 920(m, ν_{asym}(U═O)), 831(sh), 795(w), 758(w), 734(sh), 701(m), 635(m), 585(sh), 575(w), 519(w), 469-(sh), 433(w).

Synthesis of UO_2(Ar$_2$nacnac)(py)$_2$ (2). Method A. To a chilled (−25 °C) toluene solution (5 mL) of **1** (75 mg, 0.080 mmol) and py (110 μL, 1.36 mmol) was added a chilled (−25 °C) toluene solution (1 mL) of Cp_2Co (16 mg, 0.086 mmol). This resulted in a color change from orange-brown to red-purple, concomitant with the deposition of a mustard yellow powder ([Cp_2Co][OTf]). After 10 min of stirring the solution was filtered through a Celite column (2 cm × 0.5 cm) supported on glass wool. The volume of filtrate was reduced in vacuo (1 mL), and the solution was layered with hexanes (5 mL) and stored at −25 °C for 12 h. This resulted in the formation of dark purple prisms (34 mg). Yield: 50%. Anal. Calcd for $C_{39}H_{51}N_4O_2U$: C, 55.38; H, 6.08; N, 6.62. Found C, 55.40; H, 6.08; N, 6.41. ^1H NMR (400 MHz, 25 °C, C_6D_6): δ −9.27 (s, 6H, Me), −6.81 (s, 1H, γ-CH), −0.29 (s, 12H, CH*Me*$_2$), 0.76 (s, 4H, *meta* CH), 2.30 (s, 2H, *para* CH), 4.02 (br s, py), 6.63 (br s, py) 14.75 (br s, 4H, C*H*Me$_2$), 17.14 (br s, 12H, CH*Me*$_2$). One pyridine resonance was not observed. UV/vis (toluene, 2.1 × 10^{-3} M): 578 nm (ε = 400 L·mol^{-1}·cm^{-1}), 659 nm (ε = 360 L·mol^{-1}·cm^{-1}), 781 nm (ε = 290 L·mol^{-1}·cm^{-1}). IR (KBr Pellet, cm^{-1}): 1320 (m), 1264 (m), 1222 (sh), 1162 (s), 1103 (s), 1029 (s), 933 (sh), 920 (m), 840 (sh), 811(sh, ν_{asym}(U═O)), 795 (m), 759 (m), 742 (w), 704 (m), 681 (w), 627 (w), 479 (s), 429 (sh).

Method B. To a toluene (10 mL) solution of $[UO_2(Ar_2nacnac)Cl]_2$ (108 mg, 0.075 mmol) was added AgOTf (38 mg, 0.15 mmol). The solution quickly changed from green-brown to dull-red, concomitant with the deposition of a white powder. After 30 min of stirring the solution was filtered through a Celite column (2 cm × 0.5 cm) supported on glass wool, and pyridine (250 μL, 3.10 mmol) was added to the filtrate. The resulting orange-brown solution was stirred for 20 min whereupon a chilled (−25 °C) toluene solution (1 mL) of Cp_2Co (34 mg, 0.18 mmol) was added, resulting in a color change to purple-red and the deposititon of a mustard yellow powder. This solution was then filtered through a Celite column (2 cm × 0.5 cm) supported on glass wool. The volume of filtrate was reduced in vacuo (1 mL), and the solution was layered with hexanes (6 mL) and stored at −25 °C for 18 h. This resulted in the deposition of dark purple prisms (47 mg). Yield: 69%.

Synthesis of UO_2(Ar$_2$nacnac)(Bipy) (3). To a toluene (2 mL) solution of **2** (23 mg, 0.028 mmol) was added 2,2′-bipyridine (5 mg, 0.03 mmol). This resulted in an immediate color change from purple to indigo. The volume of this solution was reduced in vacuo (0.5 mL), and the solution was layered with hexanes (3 mL) and stored at −25 °C for 12 h. This resulted in the deposition of dark purple-blue prisms (19 mg). Yield: 80%. Anal. Calcd for $C_{39}H_{49}N_4O_2U$: C, 55.51; H, 5.85; N, 6.64. Found C, 54.89; H, 5.74; N, 6.50. ^1H NMR (500 MHz, 25 °C, C_6D_6): δ −44.59 (s, 2H, *6*- CH, bipy), −8.94 (s, 6H, Me), −6.93 (s, 1H, γ-CH), −3.30 (s, 2H, bipy), −1.29 (s, 2H, bipy), 0.25 (s, 12H, CH*Me*$_2$), 0.32 (s, 4H, *meta* C*H*), 1.98 (br s, 2H, bipy), 2.27 (br s, 2H, *para* C*H*), 17.39 (s, 12H, CH*Me*$_2$), 18.01 (br s, 4H, C*H*Me$_2$). UV/vis (Toluene, 1.4 × 10^{-3} M): 553 nm (ε = 460 L·mol^{-1}·cm^{-1}), 611 nm (ε = 580 L·mol^{-1}·cm^{-1}), 731 nm (ε = 140 L·mol^{-1}·cm^{-1}). IR (KBr pellet, cm^{-1}): 1319 (s), 1269 (sh), 1255 (m), 1234 (sh), 1170 (m), 1102 (w), 1059 (w), 1041 (sh), 1020 (w), 974 (w), 931 (sh), 918 (m), 898 (m), 844 (w), 819 (sh, ν_{asym}(U═O)), 794 (m), 760 (s), 746 (sh), 725 (sh), 698 (w), 654 (sh), 644 (w), 622 (w), 472 (m), 445 (sh), 426 (m).

Synthesis of UO_2(Ar$_2$nacnac)(Phen) (4). To a toluene solution (2 mL) of **2** (21 mg, 0.024 mmol) was added 1,10-phenanthroline (5 mg, 0.03 mmol). This resulted in an immediate color change from purple to indigo. The volume of this solution was reduced in vacuo (0.5 mL), and the solution was layered with hexanes (4 mL) and stored at −25 °C for 12 h. This resulted in the deposition of a dark purple solid (20 mg). Yield: 96%. Anal. Calcd for $C_{41}H_{49}N_4O_2U$: 56.74; H, 5.69; N, 6.46; Found C, 56.38; H, 5.52; N, 6.46. ^1H NMR (400 MHz, 25 °C, C_6D_6): δ −42.37 (br s, 2H, 2- CH, phen), −9.06 (s, 6H, Me), −7.02 (s, 1H, γ-CH), −2.96 (s, 2H, phen), 0.24 (s, 12H, CH*Me*$_2$), 0.31 (s, 4H, *meta*-CH), 2.43 (s, 2H, phen), 2.78 (s, 2H, *para*-CH), 3.44 (s, 2H, phen), 17.50 (s, 12H, CH*Me*$_2$), 18.26 (br s, 4H, C*H*Me$_2$). UV/vis (Toluene, 1.1 × 10^{-3} M): 554 nm (ε = 440 L·mol^{-1}·cm^{-1}), 609 nm (ε = 540 L·mol^{-1}·cm^{-1}), 735 nm (ε = 170 L·mol^{-1}·cm^{-1}). IR (KBr Pellet, cm^{-1}): 1319(s), 1273 (w), 1236 (sh), 1172 (w), 1145 (w), 1104(m), 1060 (sh), 1026 (m), 995 (sh), 932 (sh), 914 (sh), 911 (m), 902 (sh), 876 (w), 843 (m), 816 (m, ν_{asym}(U═O)), 793 (m), 760 (m), 729 (s), 703 (w), 683 (w), 640 (w), 625 (sh), 600 (sh), 488 (sh), 476 (m), 464 (sh), 454 (m), 421 (s).

Synthesis of UO_2(Ar$_2$nacnac)(TMEDA) (5). To a toluene solution (2 mL) of **2** (20 mg, 0.023 mmol) was added TMEDA (5 μL, 0.06 mmol). This resulted in an immediate color change to deep purple. The volatiles were removed in vacuo, and the resulting oil was dissolved in hexanes (1 mL). The volume of

(62) Monkowius, U.; Nogai, S.; Schmidbaur, H. *Organometallics* **2003**, *22*, 145–152.

Table 3. X-ray Crystallographic Data for Complexes **2**·C_7H_8, **3**·1/2C_7H_8, **4**, **5**, **6**·C_7H_8, **7**·CH_2Cl_2

	2·C_7H_8	**3**·1/2C_7H_8	**4**	**5**	**6**·C_7H_8	**7**·CH_2Cl_2
empirical formula	$C_{46}H_{59}N_4O_2U$	$C_{42.50}H_{53}N_4O_2U$	$C_{41}H_{49}N_4O_2U$	$C_{35}H_{57}N_4O_2U$	$C_{44}H_{61}N_6O_2U$	$C_{39}H_{55}Cl_2F_3N_6O_5SU$
crystal habit, color	prism, dark purple	plate, indigo	plate, indigo	rod, purple	Needle, purple-red	Irregular, red-purple
crystal size (mm)	0.3 × 0.15 × 0.01	0.3 × 0.3 × 0.05	0.3 × 0.3 × 0.1	0.25 × 0.05 × 0.05	0.4 × 0.05 × 0.02	0.2 × 0.2 × 0.02
crystal system	monoclinic	monoclinic	tetragonal	monoclinic	monoclinic	monoclinic
space group	$P2_1/c$	$C2/c$	$I4_1/a$	$P2_1/n$	$P2_1/n$	$P2_1/n$
volume (Å^3)	4234.4(8)	8092.6(13)	15382(8)	3635.6(13)	4188.1(12)	4447.2(7)
a (Å)	19.983(2)	37.084(3)	26.155(8)	11.126(2)	9.0558(15)	12.2732(12)
b (Å)	12.9213(15)	13.7180(14)	26.155(8)	15.594(3)	26.743(5)	21.5217(19)
c (Å)	17.4665(19)	16.9070(16)	22.486(8)	20.956(4)	17.536(3)	17.3535(16)
α (deg)	90	90	90	90	90	90
β (deg)	110.135(3)	109.795(3)	90	90.011(3)	99.541(5)	104.021(3)
γ (deg)	90	90	90	90	90	90
Z	4	8	16	4	4	4
formula weight (g/mol)	938.00	899.92	867.87	803.88	944.02	1085.88
density (calculated) (Mg/m^3)	1.471	1461	1.499	1.469	1.497	1.622
Absorption coefficient (mm^{-1})	3.874	4.050	4.259	4.498	3.918	3.877
F_{000}	1884	3552	6896	1612	1900	2160
total no. reflections	33635	30823	20820	22280	30621	36527
unique reflections	8579	8368	7434	7370	7137	8949
final R indices [$I > 2\sigma(I)$]	R1 = 0.0550	R1 = 0.0534	R1 = 0.0439	R1 = 0.0817	R1 = 0.0779	R1 = 0.0391
	wR2 = 0.1088	wR2 = 0.1240	wR2 = 0.0935	wR2 = 0.1625	wR2 = 0.1689	wR2 = 0.0731
largest diff. peak and hole (e$^-$ Å^{-3})	1.817 and −1.164	3.188 and −1.119	2.503 and −0.896	3.547 and −2.044	2.123 and −1.531	1.929 and −0.740
GOF	0.847	0.995	0.908	1.079	0.836	0.930

this solution was reduced to 0.25 mL, and the solution was stored at −25 °C for 12 h, resulting in the deposition of dark purple rods (7 mg). Yield: 34%. Anal. Calcd for $C_{35}H_{57}N_4O_2U$: C, 52.29; H, 7.15; N, 6.97; Found C, 51.96; H, 7.05; N, 6.61. ^{1}H NMR (400 MHz, 25 °C, C_6D_6): δ −17.67 (br s, 4H, CH_2), −14.70 (br s, 12H, Me_2N), −9.70 (s, 6H, Me), −8.42 (s, 1H, γ-CH), −0.23 (s, 12H, CHMe_2), 0.08 (s, 4H, *meta* CH), 1.70 (s, 2H, *para* CH), 16.66 (br s, 4H, C*H*Me$_2$), 19.03 (br s, 12H, CHMe_2). UV/vis (toluene, 3.8 × 10^{-3} M): 545 nm (ε = 550 L·mol^{-1}·cm^{-1}), 597 nm (ε = 300 L·mol^{-1}·cm^{-1}), 749 nm (ε = 85 L·mol^{-1}·cm^{-1}). IR (KBr pellet, cm^{-1}): 1320 (s), 1297 (sh), 1285 (sh), 1251 (sh), 1224 (w), 1167 (s), 1132 (w), 1104 (m), 1084 (sh), 1057 (sh), 1028 (m), 958 (w), 929 (m), 909 (sh), 820 (s, ν_{asym}(U═O)), 816(s), 790 (s), 757 (m), 719 (w), 697 (sh), 628 (w), 587 (w), 506 (sh), 472 (w), 441 (w).

Synthesis of UO$_2$(Ar$_2$nacnac)(MeIm)$_2$ (6). Method A. To a toluene solution (2 mL) of **2** (25 mg, 0.030 mmol) was added 1-methylimidazole (5 μL, 0.06 mmol). The volume of solution was reduced in vacuo (0.5 mL), and the solution was layered with hexanes (5 mL) and stored at −25 °C for 12 h, resulting in the deposition of purple-red needles (13 mg). Yield: 51%. Anal. Calcd for $C_{37}H_{53}N_6O_2U$: C, 52.17; H, 6.27; N, 9.87; Found C, 52.99; H, 5.99; N, 8.41. ^{1}H NMR (400 MHz, 25 °C, C_6D_6): δ −8.82 (s, 6H, Me), −5.90 (s, 1H, γ-H), −4.04 (br s, 2H, MeIm), −2.32 (s, 6H, NMe), −1.95 (s, 2H, MeIm), −0.11 (s, 12H, CHMe_2), 1.11 (d, 4H, J_{HH} = 6.0 Hz, *meta* CH), 2.90 (s, 2H, *para* CH), 14.14 (br s, 4H, C*H*Me$_2$), 15.46 (br s, 12H CHMe_2). One MeIm resonance was not observed. UV/vis (Toluene, 1.4 × 10^{-3} M): 530 nm (ε = 900 L·mol^{-1}·cm^{-1}), 620 nm (ε = 270 L·mol^{-1}·cm^{-1}), 758 nm (ε = 150 L·mol^{-1}·cm^{-1}). IR (KBr pellet, cm^{-1}): 1364 (m), 1320 (s), 1284 (m), 1274 (sh), 1254 (w), 1233 (m), 1164 (m), 1109 (m), 1094 (m), 1058 (w), 1045 (sh), 1027 (m), 960 (w), 934 (m), 904 (m), 857 (w), 831 (w), 810 (s, ν_{asym}-(U═O)), 804 (sh), 792 (m), 764 (m), 734 (sh), 732 (m), 696 (w), 671 (sh), 660 (m), 640 (w), 620 (w), 600 (sh), 561 (w), 507 (w), 466 (w), 438(w).

Method B. To a toluene solution (5 mL) of **7** (28 mg, 0.028 mmol) was added Cp_2Co (7 mg, 0.04 mmol). The resulting purple solution was stirred for 10 min, during which time a mustard yellow powder was deposited. This solution was filtered through a Celite column (2 cm × 0.5 cm) supported on glass wool. The volume of filtrate was reduced in vacuo (0.25 mL), and the solution was layered with hexanes (2 mL) and stored at −25 °C. This resulted in the deposition of purple red needles of **6** (7 mg). Yield: 31%.

Synthesis of [UO$_2$(Ar$_2$nacnac)(MeIm)$_2$][OTf] (7). To a dichloromethane solution (5 mL) of [UO$_2$(Ar$_2$nacnac)Cl]$_2$ (51 mg, 0.035 mmol) was added AgOTf (18 mg, 0.069 mmol). The solution quickly changed from green-brown to dull-red concomitant with the deposition of a white powder. After 30 min of stirring, the solution was filtered through a Celite column (2 cm × 0.5 cm) supported on glass wool. 1-Methylimidazole (15 μL, 0.19 mmol) was added to the filtrate, and the resulting red-orange solution was stirred for 20 min, whereupon the volume of solution was reduced in vacuo (0.5 mL), and the solution was layered with hexanes (5 mL) and stored at −25 °C for 12 h. This resulted in the deposition of red-purple crystals (42 mg). Yield: 60%. Crystals of **7** turn opaque upon application of vacuum. Anal. Calcd for $C_{38}H_{53}F_3N_6O_5SU$: C, 45.60; H, 5.34; N, 8.40. Found C, 43.18; H, 5.14; N, 8.12. ^{1}H NMR (500 MHz, 25 °C, CD_2Cl_2): δ 0.82 (d, 12H, J_{HH} = 6.0 Hz, CHMe_2), 1.18 (d, 12H, J_{HH} = 6.5 Hz, CHMe_2), 2.12 (s, 6H, Me), 3.48 (m, 4H, J_{HH} = 7.0 Hz, C*H*Me$_2$), 3.65 (s, 6H, NMe), 4.78 (s, 1H, γ-CH), 6.96 (s, 2H, Ar), 7.01 (s, 2H, Ar), 7.04 (t, 2H, J_{HH} = 8.0 Hz, *para* CH), 7.14 (s, 2H, Ar), 7.22 (d, 4H, J_{HH} = 7.5 Hz, *meta* CH). ^{19}F{^{1}H} NMR (376 MHz, 25 °C, CD_2Cl_2): δ −16.52 (s, OTf). ^{13}C{^{1}H} NMR (125 MHz, 25 °C, C_6D_6): δ 23.64 (Me), 26.93 (CHMe_2), 28.46 (CHMe_2), 28.52 (*CH*Me$_2$), 34.63 (MeN), 98.87 (γ-C), 120.95 (MeIm), 125.95, 130.58 (MeIm), 132.03, 141.89 (MeIm), 151.10 (C-ipso), 166.88 (β-C). A resonance for the CF_3 group was not observed. UV/vis (Toluene, 2.3 × 10^{-4} M): 405 nm (ε = 970 L·mol^{-1}·cm^{-1}), 496 nm (ε = 920 L·mol^{-1}·cm^{-1}), 666 nm (ε = 620 L·mol^{-1}·cm^{-1}). IR (KBr Pellet, cm^{-1}): 1388 (s), 1358 (s), 1317 (s), 1304 (sh), 1270 (s), 1232 (m), 1226 (sh), 1209 (sh), 1177 (sh), 1156 (s), 1108 (sh), 1093 (s), 1076 (sh), 1058 (w), 1032 (s), 1023 (sh), 946 (m), 932 (m), 917 (s, ν_{asym}(U═O)), 869 (w), 828 (w), 803 (sh), 793 (m), 771 (w), 753 (m), 736 (m), 698 (w), 671 (sh), 662 (w), 661 (w), 638 (s), 630 (sh), 621 (m), 574 (w), 563 (sh), 518 (m), 503 (w), 491 (w), 481 (w), 466 (w), 454 (sh), 437 (w), 429 (sh), 407 (w).

Synthesis of [UO$_2$(Ar$_2$nacnac)(Ph$_2$MePO)(MeIm)][OTf] (8). To a dichloromethane (5 mL) solution of [UO$_2$(Ar$_2$nacnac)Cl]$_2$ (54 mg, 0.037 mmol) was added AgOTf (18 mg, 0.070 mmol). The solution quickly changed from green-brown to dull-red, concomitant with the deposition of a white powder. After 30 min of stirring, the solution was filtered through a Celite

column (2 cm × 0.5 cm) supported on glass wool. Ph_2MePO (16 mg, 0.072 mmol) and 1-methylimidazole (6 μL, 0.08 mmol) were added to the filtrate, resulting in a color change to orange. After 30 min of stirring, the volume of solution was reduced in vacuo (0.5 mL), and the solution was layered with hexanes (5 mL) and stored at −25 °C for 12 h. This resulted in deposition of yellow brown powder (27 mg). Yield: 32%. Anal. Calcd for $C_{47}H_{60}F_3N_4O_6PSU$: C, 49.73; H, 5.33; N, 4.94. Found C, 49.63; H, 5.14; N, 4.68. ^{1}H NMR (400 MHz, 25 °C, C_6D_6): δ 0.81 (d, 6H, J_{HH} = 6.4 Hz, CHMe_2), 0.99 (m, 12H, CHMe_2), 1.09 (d, 6H, J_{HH} = 6.4 Hz, CHMe_2), 1.85 (m, 6H, PMe and Me), 1.90 (s, 3H, Me), 3.49 (m, 2H, J_{HH} = 6.8 Hz, C*H*Me$_2$), 3.53 (s, 3H, NMe), 3.65 (m, 2H, J_{HH} = 6.8 Hz, C*H*Me$_2$), 4.74 (s, 1H, γ CH), 6.56 (s, 1H, Ar), 6.70 (s, 1H, Ar), 6.86 (m, 2H, Ar), 6.98 (m, 3H, Ar), 7.05 (d, 2H, J_{HH} = 7.2 Hz, Ar), 7.23−7.37 (m, 10H, Ar). ^{19}F{^{1}H} NMR (376 MHz, 25 °C, C_6D_6): δ −15.06. ^{31}P{^{1}H} NMR (162 MHz, 25 °C, C_6D_6): δ 51.68. ^{13}C{^{1}H} NMR (125 MHz, 25 °C, C_6D_6): δ 14.41 (d, J_{PC} = 29 Hz, PMe), 23.76 (Me), 23.62 (Me), 26.26 (CHMe_2), 26.74 (CHMe_2), 27.62 (CHMe_2), 27.83 (CHMe_2), 28.24 (*C*HMe$_2$), 28.38 (*C*HMe$_2$), 34.60 (MeN), 98.59 (γ-C), 121.43 (MeIm), 125.80 (d, J_{PC} = 23 Hz, P-Ph), 129.06, 129.39 (d, J_{PC} = 13 Hz, P-Ph), 129.87, 129.91, 130.13, 131.63 (d, J_{PC} = 11 Hz, P-Ph), 133.63, 133.64, 134.05, 135.66, 142.24 (MeIm), 149.43 (ispo C), 149.48 (ipso C), 167.20 (β-C), 167.25 (β-C). A resonance for the CF_3 group was not observed. IR (KBr Pellet, cm^{-1}): 1388 (s), 1360 (sh), 1317 (s), 1275 (s), 1237 (m), 1225 (s), 1154 (sh), 1135 (s), 1092 (s), 1070 (sh), 1031 (s), 1000 (sh), 944 (sh), 930 (sh), 918 (s, ν_{asym}(U=O)), 893 (m), 847 (w), 833 (w), 797 (m), 786 (sh), 752 (s), 723 (w), 695 (m), 672 (w), 659 (w), 637 (s), 622 (sh), 573 (w), 513 (s), 480 (sh), 448 (sh), 437 (w), 423 (w), 414 (sh).

Competition Experiments. Ligand competition experiments were performed identically, and only a representative example is described. To a C_6D_6 (0.5 mL) solution of **2** (8 mg, 0.009 mmol) was added TMEDA (1.5 μL, 0.010 mmol). This resulted in an immediate color change from blue to dark purple. The solution was mixed for 30 s, and a ^{1}H NMR spectrum was recorded. The signals for the methyl groups attached to the β-carbons of the Ar_2nacnac ligand were integrated to determine the relative amounts of the reactant and product complexes.

(63) *SMART Software Users Guide*, 5.1; Bruker Analytical X-ray Systems, Inc.: Madison, WI, 1999.

X-ray Crystallography. The crystal structures of complexes **2**·C_7H_8, **3**·1/2C_7H_8, **4**, **5**, **6**·C_7H_8, and **7**·CH_2Cl_2 were determined similarly with exceptions noted in subsequent paragraphs. Crystals were mounted on a glass fiber under Paratone-N oil. Data collection was carried out using a Bruker 3-axis platform diffractometer with SMART-1000 CCD detector. The instrument was equipped with graphite monochromatized Mo Kα X-ray source (λ = 0.71073 Å). All data were collected at 150(2) K using Oxford nitrogen gas cryostream system. A hemisphere of data was collected using ω scans, with 25 s (for **2**·C_7H_8 and **3**·1/2C_7H_8), 15 s (for **4**), 35 s (for **5**), or 30 s (for **6**·C_7H_8 and **7**·CH_2Cl_2) frame exposures, and 0.3° frame widths. Data collection and cell parameter determination were conducted using the SMART program.[63] The raw frame data were processed using SAINT.[64] The empirical absorption correction was applied based on Psi-scan. Subsequent calculations were carried out using SHELXTL.[65] The structures was solved using Direct methods and difference Fourier techniques. All hydrogen atom positions were idealized and rode on the atom of attachment. The final refinement included anisotropic temperature factors on all non-hydrogen atoms. Structure solution, refinement, graphics, and creation of publication materials were performed using SHELXTL. A summary of relevant crystallographic data for **2**·C_7H_8, **3**·1/2C_7H_8, **4**, **5**, **6**·C_7H_8, and **7**·CH_2Cl_2 is presented in Table 3.

Acknowledgment. We thank the University of California, Santa Barbara, and the UC-National Laboratory Research Program for financial support of this work.

Supporting Information Available: ORTEP diagram of **8**, X-ray crystallographic details (as CIF files) of **2**·C_7H_8, **3**·1/2C_7H_8, **4**, **5**, **6**·C_7H_8, **7**·CH_2Cl_2, **8**·2CH_2Cl_2; UV−vis spectra for **2**, **6**; IR spectra for **1**−**8**; ^{1}H NMR spectra for ligand competition experiments. This material is available free of charge via the Internet at http://pubs.acs.org.

(64) *SAINT Software Users Guide*, Version 5.1; Bruker Analytical X-ray Systems, Inc.: Madison, WI, 1999.

(65) Sheldrick, G. M. *SHELXTL*; Bruker Analytical X-ray Systems, Inc.: Madison, WI, 2001.